Kinetic Analysis of the Interaction of Guanine Nucleotides with Eukaryotic Translation Initiation Factor eIF5B†

Vera P. Pisareva,‡ Christopher U. T. Hellen,‡ and Tatyana V. Pestova*,‡,§

Department of Microbiology and Immunology, State University of New York Downstate Medical Center, 450 Clarkson Avenue, Brooklyn, New York 11203, and A. N. Belozersky Institute of Physico-Chemical Biology, Moscow State University, Moscow, Russia

Received October 12, 2006; Revised Manuscript Received December 15, 2006

ABSTRACT: Eukaryotic translation initiation factor eIF5B is a ribosome-dependent GTPase that is responsible for the final step in initiation, which involves the displacement of initiation factors from the 40S ribosomal subunit in initiation complexes and its joining with the 60S subunit. Hydrolysis of eIF5B-bound GTP is not required for its function in subunit joining but is necessary for the subsequent release of eIF5B from assembled 80S ribosomes. Here we investigated the kinetics of guanine nucleotide binding to eIF5B by a fluorescent stopped-flow technique using fluorescent mant derivatives of GTP and GDP and of the GTP analogues GTPγS and GMPPNP. The affinity of eIF5B for mant-GTP ($K_d \sim 14-18$ μM) was approximately 7-fold less than for mant-GDP ($K_d \sim 2.3$ μM), and both guanine nucleotides dissociated rapidly from eIF5B ($k_{-1}^{\text{mant-GTP}} \sim 22-28$ s^{-1}, $k_{-1}^{\text{mant-GDP}} \sim 10-14$ s^{-1}). These properties of eIF5B suggest a rapid spontaneous GTP/GDP exchange on eIF5B and are therefore consistent with it having no requirement for a special guanine nucleotide exchange factor. The affinity of eIF5B for mant-GTPγS was about 2 times lower ($K_d \sim 6.9$ μM) and for mant-GMPPNP 1.5 times higher ($K_d \sim 25.7$ μM) than for mant-GTP, indicating that eIF5B tolerates modifications of the triphosphate moiety well.

Translation initiation in eukaryotes is a coordinated process in which at least 12 eukaryotic initiation factors (eIFs)[1] mediate the assembly of an 80S ribosomal initiation complex in which the anticodon of aminoacylated initiator tRNA (Met-tRNA$_i^{Met}$) is base-paired to the initiation codon of an mRNA in the ribosomal peptidyl (P) site (*1*). Met-tRNA$_i^{Met}$ enters this pathway as a complex with eIF2 and GTP, which together with eIF3, eIF1, and eIF1A binds to a 40S subunit to form a 43S preinitiation complex. This complex binds to the capped 5-proximal region of a mRNA whose secondary structure is unwound by the cooperative action of eIF4F, eIF4A, and eIF4B and then scans downstream to the initiation codon, where it stops and forms a 48S initiation complex with an established codon−anticodon interaction in the P-site. Initiation codon recognition and base pairing with the Met-tRNA$_i^{Met}$ anticodon triggers eIF5-mediated hydrolysis of eIF2-bound GTP (*2*, *3*) and subsequent release of phosphate (*4*), which results in a loss of affinity of eIF2 to Met-tRNA$_i^{Met}$ (*2*, *5*) and partial release of eIF2-GDP from the 40S subunit (*6*). The final step in initiation is mediated by eIF5B and involves displacement of eIF1, eIF1A, eIF3, and the remaining eIF2-GDP from the 40S subunit and joining of a 60S subunit to the 40S subunit on which Met-tRNA$_i^{Met}$ is base-paired to the initiation codon (*3*, *6*, *7*).

eIF5B and its prokaryotic homologue IF2 are universally conserved initiation factors (*8*). IF2/eIF5B is a ribosome-dependent GTPase (*7*, *9*) and consists of a divergent N-terminal region (which is not required for the activity of the eukaryotic factor) and conserved central GTP-binding (G) and C-terminal domains (*10*). The G domains of IF2 and eIF5B contain the G1−G5 sequence motifs that are characteristic of GTP-binding translation factors. Their importance for GTP binding and hydrolysis and for the factor's activity in translation have been confirmed by analysis of mutant proteins (*8*, *11*−*14*). The crystal structure of IF2/eIF5B from *Methanobacterium thermoautotrophicum* has been determined in apo-, GDP-, and GTP-bound forms (*15*). Domains I, II, and III form a globular domain that connects through a long (40 Å) α-helix to the basal domain IV. Several contacts are established between the switch 2 region of the G domain and bound Mg^{2+} and GTP (but not GDP). The bound nucleotide does not cause significant structural changes within any domain but induces rigid-body

† This work was supported by NIH Grants AI51340 to C.U.T.H. and GM63940 to T.V.P.

* To whom correspondence should be addressed. Telephone: (718) 221-6121. Fax: (718) 270-2656. E-mail: tatyana.pestova@downstate.edu.

‡State University of New York Downstate Medical Center.

§ Moscow State University.

[1] Abbreviations: ΔeIF5B, human eIF5B$_{587-1220}$; DEAE, diethylaminoethyl; dGTP, 2′-deoxyguanosine triphosphate; DTT, dithiothreitol; EDTA, ethylenediaminetetraacetic acid; EF, elongation factor; eIF, eukaryotic translation initiation factor; FPLC, fast protein liquid chromatography; FRET, fluorescence resonance energy transfer; G domain, GTPase domain of human eIF5B consisting of residues 628−850; GTPase, guanosine 5′−3′-*O*-triphosphate (GTP) binding protein; GAP, GTPase-activating protein; GEF, guanine nucleotide exchange factor; GDP, guanosine 5′-diphosphate; GMPPNP, guanosine 5′-(*β*,*γ*-imido)triphosphate; GTP, guanosine 5′-triphosphate; IF, initiation factor; K_d, equilibrium dissociation constant; mant, 2′-*O*-(*N*-methylanthraniloyl); mant-GDP, 2′/3′-*O*-(*N*-methylanthraniloyl)guanosine 5-diphosphate; mant-GTP, 2′/3′-*O*-(*N*-methylanthraniloyl)guanosine 5′-triphosphate; mant-GTPγS, 2′/3′-*O*-(*N*-methylanthraniloyl)guanosine 5′-[*γ*-thio]triphosphate; Met-tRNA$_i^{Met}$, aminoacylated initiator tRNA; NTA, nitrilotriacetic acid; P-site, peptidyl site; SDS, sodium dodecyl sulfate; Tris, tris(hydroxymethyl)aminomethane.

10.1021/bi062134g CCC: $37.00
Published on Web 02/13/2007

interdomain movements that culminate in an ~4.6 Å swinging movement of domain IV.

Human N-terminally truncated $eIF5B_{587-1220}$ is fully active in subunit joining. It assumes the active conformation on binding GTP, but whereas hydrolysis of eIF5B-bound GTP is not required for release of initiation factors from the 40S subunit and joining of it with the 60S subunit, GTP hydrolysis is required for release of eIF5B itself from the assembled 80S ribosome (*7*, *14*). This mode of action, when the protein alternates between an active GTP-bound and inactive GDP-bound state, is like that of many other GTPases, including the translation initiation factor eIF2 and the elongation factors eEF1A/EF-Tu (*16*). The requirement for a dedicated guanine nucleotide exchange factor (GEF) varies among translational GTPases. Thus, GDP/GTP exchange on eIF2 and EF-Tu requires eIF2B and EF-Ts, respectively (*17*, *18*). By contrast, no GEF that is dedicated to recycling IF2·GDP or eIF5B·GDP to the active GTP-bound form has been reported, which is consistent with the ability of eIF5B to participate in multiple rounds of ribosomal subunit joining (*7*).

Here we characterized the kinetics of interaction of full-length native rabbit eIF5B and recombinant N-terminally truncated human $eIF5B_{587-1220}$ ("ΔeIF5B") with guanine nucleotides by fluorescence stopped-flow and equilibrium fluorescence titration techniques using derivatives of GTP and GDP carrying the fluorescent methylanthraniloyl (mant) group. Both forms of eIF5B showed moderate affinities for mant-GDP and mant-GTP and fast rates of dissociation of guanine nucleotides, properties that are consistent with eIF5B not requiring a dedicated GDP/GTP exchange factor.

MATERIALS AND METHODS

Proteins. Full-length native eIF5B was purified from the 40−50% $(NH_4)_2SO_4$ saturation fraction of the 0.5 M KCl ribosomal salt wash from rabbit reticulocyte lysate (Green Hectares, Oregon, WI) by sequential chromatographies on DEAE, phosphocellulose, and a FPLC MonoQ HR5/5 column (*7*). After each step, eIF5B was dialyzed overnight against buffer A [20 mM Tris-HCl (pH 7.5), 0.1 mM EDTA, 1 mM DTT, and 5% glycerol] containing 100 mM KCl.

A hexahistidine- (His_6-) and T7-tagged N-terminally truncated human $\Delta eIF5B_{587-1220}$ fragment ("eIF5B") was expressed in *Escherichia coli* BL21(DE3). Only a minor proportion of ΔeIF5B was soluble. ΔeIF5B was first purified by chromatography on Ni^{2+}-NTA−agarose and then by FPLC chromatography on a MonoQ column (*7*, *14*). After elution from Ni^{2+}-NTA−agarose, ΔeIF5B was dialyzed overnight against buffer A containing 100 mM KCl, diluted with buffer A to a concentration of 30 mM KCl, and was then applied to a FPLC MonoQ HR5/5 column. Fractions were collected across a 30−500 mM KCl gradient; apparently homogeneous ΔeIF5B eluted with 50−70 mM KCl. The concentration of protein was determined both by the Bradford method using bovine serum albumin as a standard and spectrophotometrically at 280 nm, in which case the extinction coefficient was calculated from eIF5B's amino acid composition (*19*). The final yield of ΔeIF5B was low (~0.2 mg of ΔeIF5B/L of bacterial culture). The final preparations of both native eIF5B and ΔeIF5B did not contain guanine nucleotides as was determined by HPLC (*20*).

Fluorescence Stopped-Flow Kinetic Experiments. Stopped-flow experiments using mant-guanine nucleotides (Jena Bioscience, Jena, Germany) were done in a SX-18MV spectrometer (Applied Photophysics, Leatherhead, U.K.). Fluorescence of mant-nucleotides was excited via FRET by excitation of tryptophan at 290 nm and measured after passing through a 400 nm cutoff filter (Schott, Duryea, PA). All experiments were done in buffer B [20 mM Tris-HCl (pH 7.5), 0.1 M KCH_3COO, 2 mM DTT, and 2.5 mM $MgCl_2$] at 25 ± 1 °C. All time courses represent an average of at least seven transients. Data collection and determination of k_{app} were performed with the package from Applied Photophysics. Time curves were evaluated by fitting a single-exponential function using the equation:

$$F(t) = F_\infty + A e^{-k_{app} t}$$

where $F(t)$ is the fluorescence at time t, F_∞ is the final value of fluorescence, k_{app} is the apparent rate constant, and A is the amplitude. Association and dissociation rate constants (k_{+1} and k_{-1}, respectively) were determined from linear plots of k_{app} versus the concentration of mant-nucleotides or of protein using GraphPad Prism 4 (GraphPad Software, Inc., San Diego, CA).

Steady-State Fluorescence Measurements. Fluorescence emission spectra were recorded on a Fluoromax-3 spectrophotometer (Jobin Yvon Inc., Edison, NJ) using a 10 × 10 mm (i.d.) quartz cuvette (Bel-Art products, Pequannock, NJ) at 25 ± 1 °C. All reactions were done in buffer B. Binding of mant-nucleotides to ΔeIF5B was monitored using an excitation wavelength of 290 nm and an emission wavelength of 440 nm. To estimate the equilibrium dissociation constant, K_d, of the ΔeIF5B·mant-nucleotide complex, the fluorescence of mant-nucleotides (increasing amounts) was measured alone and in the presence of 2 μM ΔeIF5B. Dilution was less than 2%. Before measuring the fluorescence spectra, complexes were incubated in buffer B at 25 °C for 5 min. To analyze titration data, the one-site binding model was used:

$$Y = Y_{max} X/(K_d + X)$$

where X is the concentration of mant-nucleotide in the reaction and Y is the difference in the fluorescence intensities of mant-nucleotide in the presence and absence of ΔeIF5B (FRET). Y_{max} is the maximum value of FRET. Data were evaluated using GraphPad Prism 4.

The equilibrium dissociation constant for unlabeled GDP was determined by chase titration of the mant-GDP·ΔeIF5B complex (assembled with 1 μM ΔeIF5B and 5 μM mant-GDP) by increasing concentrations of GDP. The chase of mant-GDP was monitored by the change in fluorescence of the mant group (440 nm) after excitation at 297 nm. The titration data were analyzed using the model:

$$\Delta eIF5B + \text{mant-GDP} \overset{K_{\text{mant-GDP}}}{\rightleftharpoons} \Delta eIF5B\cdot\text{mant-GDP}$$

$$\Delta eIF5B + GDP \overset{K_{GDP}}{\rightleftharpoons} \Delta eIF5B\cdot GDP$$

where $K_{\text{mant-GDP}}$ and K_{GDP} are equilibrium dissociation constants of mant-GDP and GDP, respectively. In this case

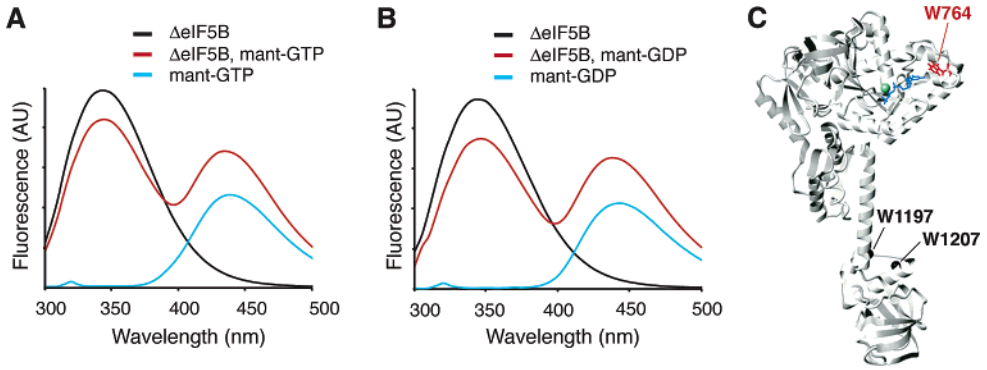

FIGURE 1: Fluorescence energy transfer between tryptophan-764 of ΔeIF5B and mant-GDP/GTP. (A) Emission spectra of 2 μM ΔeIF5B (black), 10 μM mant-GTP (blue), and their mixture (red) upon excitation at 290 nm. (B) Emission spectra of 2 μM ΔeIF5B (black), 7.5 μM mant-GDP (blue), and their mixture (red) upon excitation at 290 nm. (C) Ribbon diagram of archaeal eIF5B (*15*) (gray) with bound GMPPNP (blue) and Mg^{2+} (green). Black spheres and the red side chain represent the positions of W1197, W1207, and W764 of human eIF5B, respectively, mapped onto the crystal structure of archaeal eIF5B.

fluorescence of mant-GDP in the presence of GDP can be described by the equation:

$$F(I) = F_{max}[\text{mant-GDP}]/([\text{mant-GDP}] + K_{\text{mant-GDP}}(1 + [\text{GDP}]/K_{\text{GDP}})) + F_{min}$$

where F_{max} and F_{min} represent fluorescence intensities of ΔeIF5B·mant-GDP and mant-GDP, respectively. The equilibrium dissociation constant of GDP, K_{GDP}, was calculated by fitting the above equation to the titration data using GraphPad Prism 4.

RESULTS

Fluorescence Changes of Mant-GDP/Mant-GTP upon Binding to eIF5B. Derivatives of guanine nucleotides that contain the environmentally sensitive fluorescent mant group attached to the ribose ring have been widely used to study nucleotide binding by proteins. The compact nature of the mant group and its attachment to the 2′/3′ positions of the ribose ring account for the minimal perturbation of nucleotide−protein interactions. Fluorescence changes of the mant-nucleotide can occur upon its binding to a protein due either to a change in the polarity of the local environment of the mant group (in which case they can be monitored after direct excitation of the fluorophore) or to fluorescence resonance energy transfer (FRET) between tryptophan residues close to the nucleotide-binding site (which serve as fluorescence donors) and mant-nucleotides (which act as acceptors) after excitation of tryptophan residues (*21*, *22*). Binding of mant-nucleotides to ΔeIF5B did not result in fluorescence changes upon direct excitation of the mant group at 349 nm (data not shown). However, after tryptophan excitation at 290 nm, substantial energy transfer was observed between tryptophan residues of ΔeIF5B and mant groups in ΔeIF5B·mant-GTP, ΔeIF5B·mant-GDP, ΔeIF5B·mant-dGTP, ΔeIF5B·mant-GTPγS, and ΔeIF5B·mant-GMPPNP complexes, which was manifested as a simultaneous decrease in tryptophan fluorescence and an increase in mant fluorescence compared to the protein alone and free mant-nucleotides (Figure 1A,B; data not shown). The only tryptophan residue in the G domain of human ΔeIF5B is W764, about 20 Å from the nucleotide-binding site, which is sufficiently close to contribute to FRET (*15*). Other tryptophan residues (W1197 and W1207) in ΔeIF5B are in domain IV, over 50 Å from the nucleotide-binding site, and would make a negligible contribution to FRET. The observed FRET is therefore likely the result of energy transfer between the bound mant-nucleotide and W764 of ΔeIF5B.

Interaction of N-Terminally Truncated Recombinant ΔeIF5B and Full-Length Native eIF5B with Mant-GDP and Mant-GTP. The kinetics of binding of mant-guanine nucleotides to full-length native rabbit eIF5B and recombinant human ΔeIF5B (Figures 2−4) was measured by fluorescence stopped flow, monitoring fluorescence changes of the mant-nucleotide upon its binding to the factor after indirect excitation at 290 nm via FRET from W764 of ΔeIF5B to the mant group.

The kinetics of association of mant-GDP to ΔeIF5B (Figure 2A−C) was measured under pseudo-first-order conditions (1 μM eIF5B and 5−10 μM mant-GDP). The time courses in this (Figure 2A) and all other experiments described below were fitted by a single-exponential term, yielding pseudo-first-order rate constants, k_{app}, that were linearly dependent on the mant-nucleotide concentration (Figure 2C). This behavior is consistent with a simple one-step binding model:

$$\Delta\text{eIF5B} + \text{mant-GDP} \underset{k_{-1}}{\overset{k_{+1}}{\rightleftharpoons}} \Delta\text{eIF5B·mant-GDP}$$

The association and dissociation rate constants k_{+1} and k_{-1} can be determined from the linear concentration dependence of k_{app} using the equation:

$$k_{app} = k_{+1}[\text{mant-GDP}] + k_{-1}$$

The slope of the straight line fitted to the data points defines k_{+1} (M^{-1} s^{-1}), and the intercept with the *y*-axis yields k_{-1} (s^{-1}). The value of k_{-1} was also determined in a displacement experiment in which a 50-fold molar excess of unlabeled GDP was used to displace mant-GDP from the ΔeIF5B·mant-GDP complex (Figure 2B), but although this value is shown in Figure 2C, it was not used for fitting the data points. The time course of mant-GDP displacement was also fitted by a single-exponential term, yielding the dissociation rate constant k_{-1}. The values of the association and dissociation rate constants ($k_{+1} = 5.6$ μM^{-1} s^{-1}, $k_{-1} = 13.6$ s^{-1}) derived from the concentration dependence of k_{app} yielded a value of ~2.4 μM for the equilibrium dissociation constant, K_d

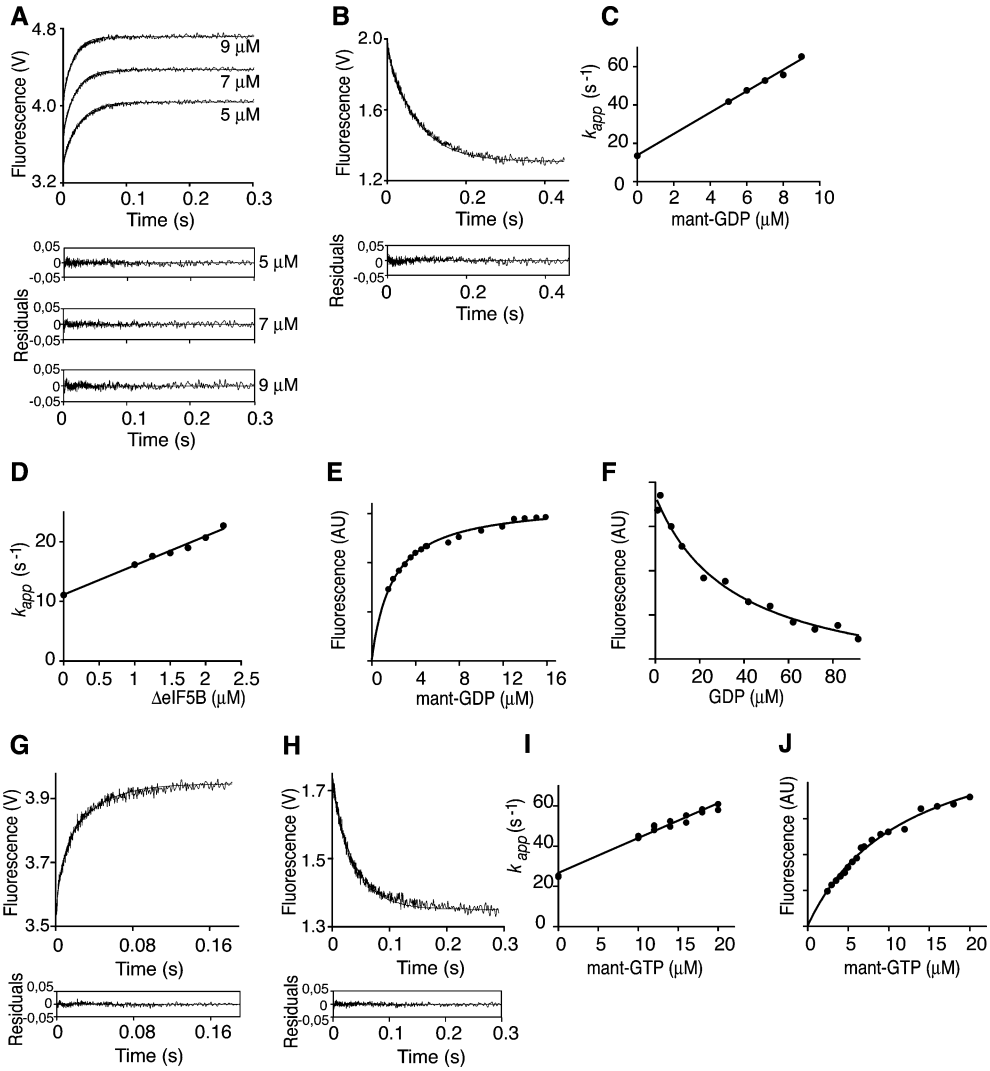

FIGURE 2: Binding of mant-GDP, mant-GTP, and GDP to ΔeIF5B. Time courses of (A) the association of mant-GDP (5, 7, and 9 μM) with ΔeIF5B (1 μM) and (B) the dissociation of mant-GDP from the mant-GDP·ΔeIF5B complex (8 μM mant-GDP and 1 μM ΔeIF5B) in the presence of GDP (400 μM). The smooth lines represent single-exponential fits that yielded the respective rate constants k_{app}. (C) Dependence of k_{app} values for mant-GDP·ΔeIF5B association on mant-GDP concentration. (D) Dependence of k_{app} values for ΔeIF5B·mant-GDP association on ΔeIF5B concentration. (E) Titration of ΔeIF5B (0.5 μM) with mant-GDP. The solid line shows the fit to the data using a one-site binding model. (F) Chase titration of the mant-GDP·ΔeIF5B complex (1 μM ΔeIF5B and 5 μM mant-GDP) with GDP. The solid line represents the result of the fit as described in Materials and Methods. Time courses of (G) the association of mant-GTP (10 μM) with ΔeIF5B (2 μM) and (H) the dissociation of mant-GTP from the ΔeIF5B·mant-GTP complex (16 μM mant-GTP and 2 μM ΔeIF5B) in the presence of GTP (800 μM). The smooth lines represent single-exponential fits that yielded the respective rate constants k_{app}. (I) Dependence of k_{app} values for ΔeIF5B·mant-GTP association on mant-GTP concentration. (J) Titration of ΔeIF5B (0.5 μM) with mant-GTP. The solid line shows the fit to the data using a one-site binding model. (A, B, G, H) Residuals for the fits of the time courses are shown in the lower panels.

(Table 1). Despite the very low yield of purified ΔeIF5B, the affinity of ΔeIF5B to mant-GDP was sufficient to perform reciprocal kinetic studies, in which the mant-GDP concentration (0.2 μM) remained constant and that of ΔeIF5B varied (time courses are not shown). The values for the association and dissociation rate constants (Table 1) calculated from the concentration dependence of k_{app} (Figure 2D) and resulting value for the K_d of ~2.3 μM were virtually identical (within the range of experimental error) to those obtained in titration studies done at a constant concentration of ΔeIF5B with varying excess concentrations of mant-GDP (Table 1). The value of K_d calculated from kinetic measurements was also identical to the K_d value obtained by equilibrium titration (Figure 2E, Table 1). The K_d value of ~6.2 μM for binding of unlabeled GDP to ΔeIF5B was determined by titrating the ΔeIF5B·mant-GDP complex with GDP (Figure 2F). However, we note that this measurement might not be completely accurate because of the substantial observed quenching of the fluorescence of tryptophans due to the inner filter effect caused by high concentrations of GDP.

The kinetics of binding of mant-GTP to ΔeIF5B was also measured under pseudo-first-order conditions (2 μM ΔeIF5B and 10−20 μM mant-GTP; Figure 2G−I). The apparent rate constants of binding were linearly dependent on the mant-GTP concentration (Figure 2I). The time course of mant-GTP displacement from the binary complex by excess GTP was also fitted by a single-exponential term (Figure 2H), yielding the dissociation rate constant k_{-1}. The values of k_{+1} = 1.7 μM^{-1} s^{-1} and k_{-1} = 28.4 s^{-1} yielded a value of ~16.9 μM for the K_d (Table 1) that agreed well with the K_d value of ~14.2 μM obtained by equilibrium titration (Figure 2J,

Table 1: Rate Constants and Equilibrium Dissociation Constants of the Interaction between Mant-guanine Nucleotides and eIF5B Determined by Fluorescence Stopped Flow

protein	nucleotide	k_{+1} (mM^{-1} s^{-1})	k_{-1} (s^{-1})	K_d (mM)
ΔeIF5B	mant-GDP	5.6 ± 0.2	13.6 ± 1.4	2.4 ± 0.3[a]
		4.9 ± 0.3	11.1 ± 0.4	2.3 ± 0.1[b]
				2.3 ± 0.3[c]
ΔeIF5B	mant-GTP	1.7 ± 0.1	28.4 ± 1.8	16.9 ± 1.7[a]
				14.2 ± 2[c]
eIF5B	mant-GDP	4.3 ± 0.2	9.6 ± 1.5	2.3 ± 0.4[a]
eIF5B	mant-GTP	1.5 ± 0.1	21.8 ± 0.9	14.5 ± 1.1[a]
ΔeIF5B	mant-dGTP	0.9 ± 0.1	30.4 ± 1.2	32.2 ± 3.6[a]
ΔeIF5B	mant-GTPγS	1.4 ± 0.1	9.8 ± 0.6	6.8 ± 0.5[a]
ΔeIF5B	mant-GMPPNP	0.6 ± 0.3	14.9 ± 0.9	25.7 ± 4.7[a]
ΔeIF5B	GDP			6.2 ± 1.2[d]

[a] Determined by fluorescence stopped flow at a constant concentration of eIF5B. [b] Determined by fluorescence stopped flow at a constant concentration of mant-GDP. [c] Determined by equilibrium fluorescence titration. [d] Determined by chase titration.

Table 1). The affinity of ΔeIF5B for mant-GTP was therefore about 7 times lower than for mant-GDP. Unfortunately, it was impossible to measure the binding of unlabeled GTP to ΔeIF5B reliably by chase titration because of the severe quenching of the fluorescence of tryptophans caused by the even higher (compared to GDP) concentrations of unlabeled GTP required for titration due to its lower affinity to ΔeIF5B.

The kinetics of association of mant-GDP and mant-GTP to full-length native eIF5B was also measured under pseudo-first-order conditions (1 μM eIF5B and 5−15 μM mant-GDP/mant-GTP) (Figure 3). The apparent rate constants of binding were linearly dependent on the concentrations of mant-GDP (Figure 3C) and mant-GTP (Figure 3F). The values of k_{-1} were determined in displacement experiments (Figure 3B,E). The determined values for the association and dissociation rate constants (k_{+1} = 4.3 μM^{-1} s^{-1}, k_{-1} = 9.6 s^{-1}) and calculated value of ~2.3 μM for the equilibrium dissociation constant K_d (Table 1) for binding of mant-GDP to native eIF5B were very similar to those obtained for recombinant ΔeIF5B (Table 1). The values for the association rate constant (k_{+1} = 1.5 μM^{-1} s^{-1}), the dissociation rate constant (k_{-1} = 21.8 s^{-1}), and the equilibrium dissociation constant (K_d = 14.5 μM) for binding of mant-GTP to full-length native eIF5B were also very similar to values obtained for recombinant N-terminally truncated ΔeIF5B (Table 1). The nonessential N-terminal domain of eIF5B does not therefore contribute to the protein's affinity to guanine nucleotides.

These results indicate that the affinity of eIF5B for mant-GTP (K_d ~ 14.2−18.3 μM) is less than an order of magnitude lower than for mant-GDP (K_d ~ 2.3−2.4 μM) and that both nucleotides dissociate rapidly from eIF5B (k_{-1}^{GTP} ~ 22−28 s^{-1}, k_{-1}^{GDP} ~ 10−14 s^{-1}).

Interaction of Mant-dGTP, Mant-GTPγS, and Mant-GMPPNP with Recombinant ΔeIF5B. To investigate the influence of the absence of the 2′-OH group of the ribose ring and of the modifications of the triphosphate moiety on

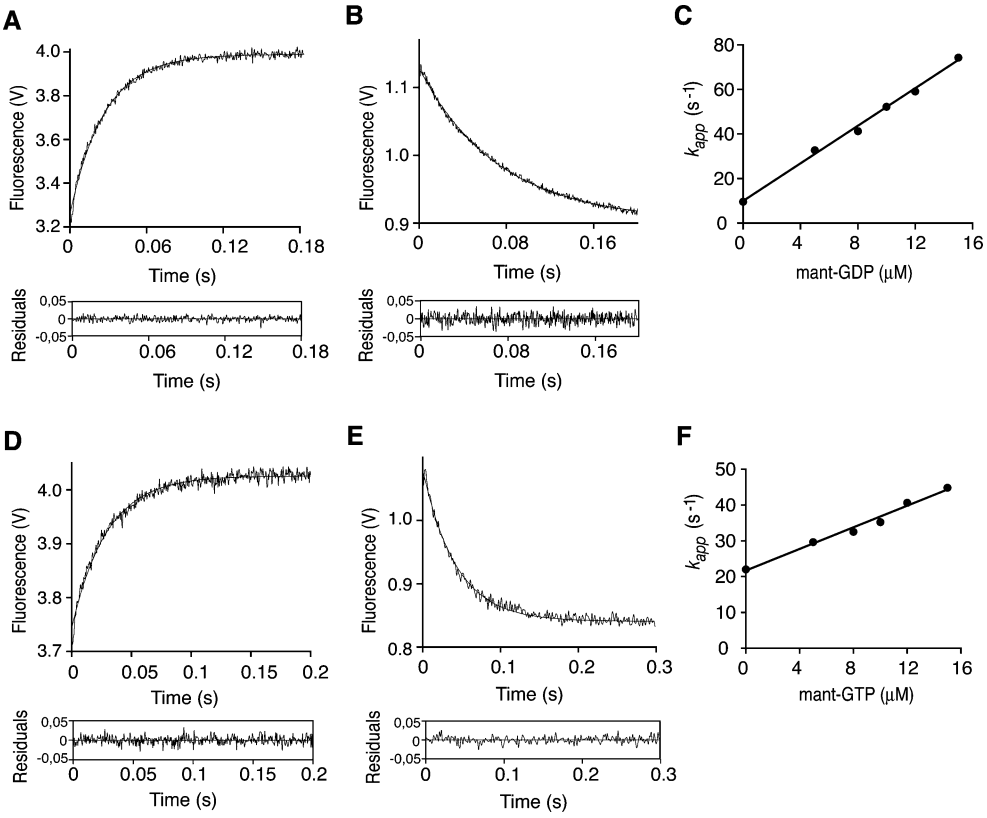

FIGURE 3: Binding of mant-GDP and mant-GTP to native full-length eIF5B. Time courses of (A) the association of mant-GDP (5 μM) with eIF5B (1 μM) and (B) the dissociation of mant-GDP from the eIF5B·mant-GDP complex (10 μM mant-GDP and 1 μM eIF5B) in the presence of GDP (500 μM). The smooth lines represent single-exponential fits that yielded the respective rate constants k_{app}. (C) Dependence of k_{app} values for eIF5B·mant-GDP association on mant-GDP concentration. Time courses of (D) the association of mant-GTP (10 μM) with eIF5B (1 μM) and (E) the dissociation of mant-GTP from the eIF5B·mant-GTP complex (10 μM mant-GTP and 1 μM eIF5B) in the presence of GTP (500 μM). The smooth lines represent single-exponential fits that yielded the respective rate constants k_{app}. (F) Dependence of k_{app} values for eIF5B·mant-GTP association on mant-GTP concentration. (A, B, D, E) The lower panels represent residuals for the fits of the time courses.

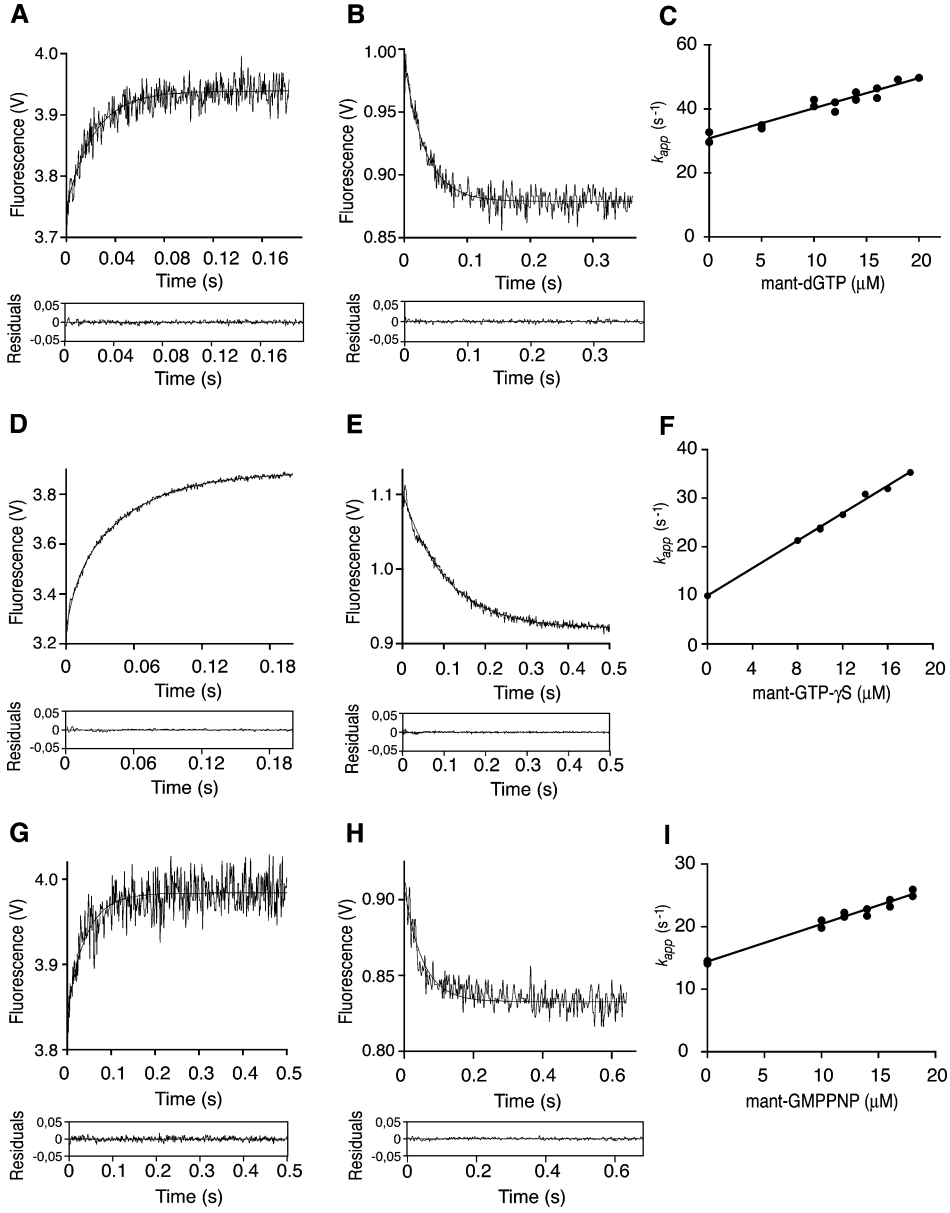

FIGURE 4: Binding of mant-dGTP, mant-GTPγS, and mant-GMPPNP to ΔeIF5B. Time courses of (A) the association of mant-dGTP (10 μM) with ΔeIF5B (2 μM) and (B) the dissociation of mant-dGTP from the ΔeIF5B·mant-dGTP complex (15 μM mant-dGTP and 2 μM ΔeIF5B) in the presence of dGTP (750 μM). The smooth lines represent single-exponential fits that yielded the respective rate constants k_{app}. (C) Dependence of k_{app} values for ΔeIF5B·mant-dGTP association on mant-dGTP concentration. Time courses of (D) the association of mant-GTPγS (10 μM) with ΔeIF5B (2 μM) and (E) the dissociation of mant-GTPγS from the ΔeIF5B·mant-GTPγS complex (14 μM mant-GTPγS and 2 μM ΔeIF5B) in the presence of GTPγS (700 μM). The smooth lines represent single-exponential fits that yielded the respective rate constants k_{app}. (F) Dependence of k_{app} values for ΔeIF5B·mant-GTPγS association on mant-GTPγS concentration. Time courses of (G) the association of mant-GMPPNP (10 μM) with ΔeIF5B (2 μM) and (H) the dissociation of mant-GMPPNP from the ΔeIF5B·mant-GMPPNP complex (14 μM mant-GMPPNP and 2 μM ΔeIF5B) in the presence of GMPPNP (700 μM). The smooth lines represent single-exponential fits that yielded the respective rate constants k_{app}. (I) Dependence of k_{app} values for ΔeIF5B·mant-GMPPNP association on mant-GMPPNP concentration. (A, B, D, E, G, H) Residuals for the fits of the time courses are shown in the lower panels.

the binding of guanine nucleotides to eIF5B, we studied the kinetics of binding mant-dGTP, the slowly hydrolyzable GTP analogue mant-GTPγS, and the nonhydrolyzable analogue mant-GMPPNP to ΔeIF5B.

The kinetics of mant-dGTP binding to ΔeIF5B was assayed under pseudo-first-order conditions (2 μM ΔeIF5B and concentrations of mant-dGTP from 5 to 20 μM; Figure 4A−C). The value of k_{-1} was determined more accurately in a displacement experiment analogous to those described above. The apparent rate constants of binding were linearly dependent on the concentrations of mant-dGTP (Figure 4C). The calculated values for k_{+1}, k_{-1}, and K_d were 0.9 μM^{-1} s^{-1}, 30.4 s^{-1}, and 32.2 μM, respectively (Table 1). The affinity of eIF5B for mant-dGTP was therefore about 2-fold lower than for mant-GTP. Although mant-GDP/mant-GTP consists of mixtures of the 2′- and 3′-*O*-methylanthraniloyl isomers that do not always bind identically to guanine nucleotide binding proteins (e.g., ref *23*), the kinetics of mant-GDP/GTP binding to eIF5B did not indicate that the two isomers bind to eIF5B with different affinities, and therefore the lower affinity of ΔeIF5B to mant-dGTP is most likely not due to the lower affinity of the 3′-*O*-methylanthraniloyl isomer but is instead due to the low stimulatory influence of the 2′-OH group on binding of mant-GTP to eIF5B.

Finally, the kinetics of association of ΔeIF5B with the slowly hydrolyzable GTP analogue mant-GTPγS and the nonhydrolyzable analogue mant-GMPPNP was measured under pseudo-first-order conditions (2 μM ΔeIF5B and 8−18 μM mant-GTPγS/mant-GMPPNP; Figure 4D−I). The linear dependency of apparent rate constants on concentrations of mant-GTPγS/mant-GMPPNP (Figure 4F,I) indicated that the binding of these mant-nucleotides to eIF5B could also be described by a one-step binding mechanism. The association and dissociation rate constants determined from the linear plots and the calculated $K_d = 6.9$ μM for the complex of mant-GTPγS with ΔeIF5B and $K_d = 25.7$ μM for the ΔeIF5B·mant-GMPPNP complex (Table 1) indicated that mant-GTPγS bound to eIF5B ~2 times more strongly than mant-GTP, mostly due to a slower rate of dissociation, whereas binding of mant-GMPPNP to ΔeIF5B was 1.8-fold weaker, mostly due to a slower rate of association.

DISCUSSION

Data reported here indicate that the affinity of human eIF5B for mant-GTP ($K_d \sim 14-18$ μM) is less than an order of magnitude lower than for mant-GDP ($K_d \sim 2.3$ μM) and that both nucleotides dissociate rapidly from eIF5B ($k_{-1}^{GTP} \sim 22-28$ s^{-1}, $k_{-1}^{GDP} \sim 10-14$ s^{-1}). Fast rates for dissociation from, as well as for association of, GDP and GTP with eIF5B account for there being no requirement for a guanine nucleotide exchange factor (GEF) for GDP/GTP exchange on eIF5B. The similarity in eIF5B's affinities for GDP and GTP suggests that, at physiological concentrations of GTP (305 μM) and GDP (36 μM) in human cells (*24*), eIF5B will spontaneously dissociate from GDP after release from the assembled ribosome and readily rebind GTP.

The affinity of eIF5B for mant-GTP and mant-GDP was also similar to the affinity of its bacterial homologue IF2 to GDP and GTP assayed by equilibrium dialysis at 5 °C ($K_d^{GDP} \sim 4$ μM and $K_d^{GTP} \sim 37$ μM; *25*) and to mant-GTP assayed by fluorescence stopped flow at 20 °C ($K_d^{mant-GTP} \sim 40$ μM; *26*). It was previously reported that the binding of GTP, but not GDP, to IF2 can be strongly stimulated by the simultaneous presence of fMet-tRNA$_i^{Met}$ and 30S subunits ($K_d \sim 2$ μM) (*27*). Although, unlike IF2, eIF5B does not form a ternary complex with GTP and initiator tRNA in solution and is not involved in binding of initiator tRNA to the small ribosomal subunit, it is possible that eIF5B might interact with initiator tRNA at a later stage in eukaryotic initiation, after eIF5-stimulated hydrolysis of eIF2-bound GTP. Thus, we recently found that, even in the absence of 60S subunits, eIF5B facilitates release of eIF2-GDP from the 40S subunit in initiation complexes (*6*). We therefore cannot exclude the possibility that binding of eIF5B to the 48S initiation complex after eIF5-induced hydrolysis of eIF2-bound GTP might also specifically increase the relatively low affinity of eIF5B for GTP. That ribosomes and functional translational ribosomal complexes influence the affinities of translation factors for GTP/GDP is not unusual. Thus, prokaryotic ribosomal posttermination complexes act as the GEF for release factor RF3 (*28*), whereas 80S ribosomes increase the affinity of rat liver and *Sulfolobus solfataricus* EF2 for GTP or analogues thereof (but not for GDP) (*29*, *30*), and 70S ribosomes strongly increase the affinity of EF-G to both GTP and GDP (*31*, *32*) likely by closing the nucleotide-binding pocket, as suggested by Wilden et al. (*32*).

The affinities of translational GTPases to GTP and its nonhydrolyzable analogue GMPPNP can differ. Thus, the affinity of EF-G for mant-GMPPNP is about 6 times lower than for GTP (*32*), and according to recent data, eukaryotic release factor eRF1 has a strong stimulatory effect on binding of GTP, but not GMPPNP, to eukaryotic release factor eRF3 (*33*). It has recently been suggested that GMPPNP might be a poor GTP analogue for eIF5B (*33*), based on the crystal structure of the complex of archaeal eIF5B with GMPPNP, in which binding of this guanine nucleotide caused relatively small structural changes in the G domain (*15*) that do not lead to coordination of the γ-phosphate by the invariant Thr residue of switch 1 and the Gly residue of switch 2 (Thr-665 and Gly-705 in human eIF5B) that is characteristic of the crystal structures of other GTPase·GTP complexes (reviewed in ref *34*). Contrary to this suggestion, we found that the affinity of eIF5B for GMPPNP was only less than 2 times lower than for GTP. However, we cannot exclude the possibility that binding of the ribosome to eIF5B in initiation complexes might induce local conformational changes in its G domain that result in greater differences between eIF5B's affinity for GTP and GMPPNP. The role of the ribosome in binding of guanine nucleotides to eIF5B would be an interesting subject for further investigation.

ACKNOWLEDGMENT

We thank all members of the Pestova and Hellen laboratories for valuable suggestions and comments on the manuscript.

REFERENCES

1. Pestova, T. V., Kolupaeva, V. G., Lomakin, I. B., Pilipenko, E. V., Shatsky, I. N., Agol, V. I., and Hellen, C. U. T. (2001) Molecular mechanisms of translation initiation in eukaryotes, *Proc. Natl. Acad. Sci. U.S.A. 98*, 7029−7036.
2. Das, S., and Maitra, U. (2001) Functional significance and mechanism of eIF5-promoted GTP hydrolysis in eukaryotic translation initiation, *Prog. Nucleic Acid Res. Mol. Biol. 70*, 207−231.
3. Unbehaun, A., Borukhov, S. I., Hellen, C. U. T., and Pestova, T. V. (2003) Release of initiation factors from 48S complexes during ribosomal subunit joining and the link between establishment of codon-anticodon base-pairing and hydrolysis of eIF2-bound GTP, *Genes Dev. 18*, 3078−3093.
4. Algire, M. A., Maag, D., and Lorsch, J. R. (2005) Pi release from eIF2, not GTP hydrolysis, is the step controlled by start-site selection during eukaryotic translation initiation, *Mol. Cell 20*, 251−262.
5. Kapp, L. D., and Lorsch, J. R. (2004) GTP-dependent recognition of the methionine moiety on initiator tRNA by translation factor eIF2, *J. Mol. Biol. 335*, 923−936.
6. Pisarev, A. V., Kolupaeva, V. G., Pisareva, V. P., Merrick, W. C., Hellen, C. U. T., and Pestova, T. V. (2006) Specific functional interactions of nucleotides at key −3 and +4 positions flanking the initiation codon with components of the mammalian 48S translation initiation complex, *Genes Dev. 20*, 624−636.
7. Pestova, T. V., Lomakin, I. B., Lee, J. H., Choi, S. K., Dever, T. E., and Hellen, C. U. T. (2000) The joining of ribosomal subunits in eukaryotes requires eIF5B, *Nature 403*, 332−335.
8. Lee, J. H., Choi, S. K., Roll-Mecak, A., Burley, S. K., and Dever, T. E. (1999) Universal conservation in translation initiation revealed by human and archaeal homologs of bacterial translation initiation factor IF2, *Proc. Natl. Acad. Sci. U.S.A. 96*, 4342−4347.
9. Kolakofsky, D., Dewey, K. F., Hershey, J. W. B., and Thach, R. E. (1968) Guanosine 5′-triphosphatase activity of initiation factor f2, *Proc. Natl. Acad. Sci. U.S.A. 61*, 1066−1070.
10. Pestova, T. V., Dever, T. E., and Hellen, C. U. T. (2000) Ribosomal subunit joining, in *Translational Control of Gene Expression* (Sonenberg, N., Hershey, J. W. B., and Mathews, M.

B., Eds.) pp 425−445, Cold Spring Harbor Laboratory Press, Cold Spring Harbor, NY.
11. Laalami, S., Timofeev, A. V., Putzer, H., Leautey, J., and Grunberg-Manago, M. (1994) In vivo study of engineered G-domain mutants of Escherichia coli translation initiation factor IF2, *Mol Microbiol. 11*, 293−302.
12. Luchin, S., Putzer, H., Hershey, J. W., Cenatiempo, Y., Grunberg-Manago, M., and Lalaami, S. (1999) In vitro study of two dominant inhibitory GTPase mutants of *Escherichia coli* translation initiation factor 2. Direct evidence that GTP hydrolysis is necessary for factor recycling, *J. Biol. Chem. 274*, 6074−6079.
13. Laursen, B. S., Siwanowicz, I., Larigauderie, G., Hedegaard, J., Ito, K., Nakamura, Y., Kenney, J. M., Mortensen, K. K., and Sperling-Petersen, H. U. (2003) Characterization of mutations in the GTP-binding domain of IF22 resulting in cold-sensitive growth of *Escherichia coli*, *J. Mol. Biol. 326*, 543−551.
14. Lee, J. H., Pestova, T. V., Shin, B. S., Cao, C., Choi, S. K., and Dever, T. E. (2002) Initiation factor eIF5B catalyzes second GTP-dependent step in eukaryotic translation initiation, *Proc. Natl. Acad. Sci. U.S.A. 99*, 16689−16694.
15. Roll-Mecak, A., Cao, C., Dever, T. E., and Burley, S. K. (2000) X-Ray structures of the universal translation initiation factor IF2/eIF5B: conformational changes on GDP and GTP binding, *Cell 103*, 781−792.
16. Kubarenko, A. V., Sergiev, P. V., and Rodnina, M. V. (2005) GTPases of the translational apparatus, *Mol. Biol. (Moscow) 39*, 746−761.
17. Panniers, R., Rowlands, A. G., and Henshaw, E. G. (1988) The effect of Mg^{2+} and guaninine nuclotide exchange factor on the binding of guanine nucleotides to eukaryotic initiation factor 2, *J. Biol. Chem. 263*, 5519−5525.
18. Gromadski, K. B., Wieden, H. J., and Rodnina, M. V. (2002) Kinetic mechanism of elongation factor Ts-catalyzed nucleotide exchange in elongation factor Tu, *Biochemistry 41*, 162−169.
19. Gill, S. C., and von Hippel, P. H. (1989) Calculation of protein extinction coefficients from amino acid sequence data, *Anal. Biochem. 182*, 319−326.
20. Hemsath, L., and Ahmadian, M. R. (2005) Fluorescence approaches for monitoring interactions of Rho GTPases with nucleotides, regulators, and effectors, *Methods 37*, 173−178.
21. John, J., Sohmen, R., Feuerstein, J., Linke, R., Wittinghofer, A., and Goody, R. S. (1990) Kinetics of interaction of nucleotides with nucleotide-free H-ras p21, *Biochemistry 29*, 6058−6065.
22. Rodnina, M. V., Fricke, R., Kuhn, L., and Wintermeyer, W. (1995) Codon-dependent conformational change of elongation factor Tu preceding GTP hydrolysis on the ribosome, *EMBO J. 14*, 2613−2619.
23. Rensland, H., Lautwein, A., Wittinghofer, A., and Goody, R. S. (1991) Is there a rate-limiting step before GTP cleavage by H-ras p21?, *Biochemistry 30*, 11181−11185.
24. Traut, T. W. (1994) Physiological concentrations of purines and pyrimidines, *Mol. Cell. Biochem. 140*, 1−22.
25. Pon, C. L., Paci, M., Pawlik, R. T., and Gualerzi, C. O. (1985) Structure-function relationship in *Escherichia coli* initiation factors. Biochemical and biophysical characterization of the interaction between IF-2 and guanosine nucleotides, *J. Biol. Chem. 260*, 8918−8924.
26. Milon, P., Tischenko, E., Tomsic, J., Caserta, E., Folkers, G., La Teana, A., Rodnina, M. V., Pon, C. L., Boelens, R., and Gualerzi, C. O. (2006) The nucleotide-binding site of bacterial translation initiation factor 2 (IF2) as a metabolic sensor, *Proc. Natl. Acad. Sci. U.S.A. 103*, 13962−13967.
27. Antoun, A., Pavlov, M. Y., Andersson, K., Tenson, T., and Ehrenberg, M. (2003) The roles of initiation factor 2 and guanosine triphosphate in initiation of protein synthesis, *EMBO J. 22*, 5593−5601.
28. Zavialov, A. V., Buckingham, R. H., and Ehrenberg, M. (2001) A posttermination ribosomal complex is the guanine nucleotide exchange factor for peptide release factor RF3, *Cell 107*, 115−124.
29. Nurten, R., and Bermek, E. (1980) Interactions of elongation factor 2 (EF-2) with guanine nucleotides and ribosomes. Binding of periodate-oxidized guanine nucleotides to EF-2, *Eur. J. Biochem. 103*, 551−555.
30. Raimo, G., Masullo, M., and Bocchini, V. (1995) Studies on the polypeptide elongation factor 2 from *Sulfolobus solfataricus*. Interaction with guanosine nucleotides and GTPase activity stimulated by ribosomes, *J. Biol. Chem. 270*, 21082−21085.
31. Baca, O. G., Rohrbach, M. S., and Bodley, J. W. (1976) Equilibrium measurements of the interactions of guanine nucleotides with *Escherichia coli* elongation factor G and the ribosome, *Biochemistry 15*, 4570−4574.
32. Wilden, B., Savlesbergh, A., Rodnina, M. V., and Wintermeyer, W. (2006) Role and timing of GTP binding and hydrolysis during EF-G-dependent tRNA translocation on the ribosome, *Proc. Natl. Acad. Sci. U.S.A. 103*, 13670−13675.
33. Hauryliuk, V., Zavialov, A, Kisselev, L., and Ehrenberg, M. (2006) Class-1 release factor eRF1 promotes GTP binding by class-2 release factor eRF3, *Biochimie 88*, 747−457.
34. Vetter, I. R., and Wittinghofer, A. (2001) The guanine nucleotide-binding switch in three dimensions, *Science 294*, 1299−1304.

BI062134G